

# An Analysis of Electron Donor–Acceptor Complexes: $\text{H}_2\text{O}\cdot\text{F}_2$ , $\text{H}_2\text{O}\cdot\text{Cl}_2$ , and $\text{H}_2\text{O}\cdot\text{ClF}$

T. Dahl\* and I. Røeggen

Contribution from the Institute of Mathematical and Physical Sciences, University of Tromsø, N-9037 Tromsø, Norway

Received November 13, 1995. Revised Manuscript Received February 21, 1996<sup>⊗</sup>

**Abstract:** An extended geminal model has been applied to study the electron donor-acceptor complexes  $\text{H}_2\text{O}\cdot\text{F}_2$ ,  $\text{H}_2\text{O}\cdot\text{Cl}_2$  and  $\text{H}_2\text{O}\cdot\text{ClF}$ . By adopting a [9s, 6p, 4d, 2f/8s, 5p, 4d, 2f/4s, 3p, 1d] contracted Gaussian-type basis set, the equilibrium O–X (X nearest halogen atom) distances are predicted to be 2.69, 2.84, and 2.60 Å, and the binding energies to be 5.86, 12.51, and 20.24 kJ/mol for the complexes  $\text{H}_2\text{O}\cdot\text{F}_2$ ,  $\text{H}_2\text{O}\cdot\text{Cl}_2$ , and  $\text{H}_2\text{O}\cdot\text{ClF}$ , respectively. The halogen molecule is situated in the plane of the  $\text{H}_2\text{O}$  molecule in the  $\text{H}_2\text{O}\cdot\text{F}_2$  complex, whereas it points approximately toward a lone pair of the O atom in the  $\text{H}_2\text{O}\cdot\text{Cl}_2$  and  $\text{H}_2\text{O}\cdot\text{ClF}$  complexes. The charge centroid of the corresponding lone pair geminal is moved considerably toward the halogen molecule as a result of the complex formation in the two latter complexes. Two slightly different decomposition schemes for the potential are considered. For the equilibrium structures the Coulombic interaction between the distorted monomers has the largest magnitude within the primary decomposition scheme, and the potential is not very different from the intermolecular correlation energy.

## I. Introduction

Molecular complexes between halogens and molecules containing oxygen belong to the class of complexes called charge-transfer complexes or electron donor-acceptor complexes. A general theory for charge-transfer complexes was formulated in 1952 by Mulliken.<sup>1</sup> The nature of such complexes, in particular the contribution of charge-transfer forces relative to other kinds of intermolecular forces to the ground-state stabilization has been a subject of dispute.<sup>2,3</sup>

Closely related to the halogen complexes with oxygen-containing donor molecules are those with nitrogen-containing donor molecules. In an earlier paper we have reported the results of quantum mechanical studies based on an extended geminal model of complexes between  $\text{NH}_3$  and  $\text{F}_2$ ,  $\text{Cl}_2$  and  $\text{ClF}$ .<sup>4</sup> In these studies intermolecular distances were obtained which are shorter than those obtained in most of the quantum-mechanical studies performed earlier for these complexes. At that time no experimental distance had been reported for any of these complexes, but from the general trends observed for similar complexes in X-ray studies it was anticipated that the  $\text{NH}_3\cdots\text{Cl}_2$  distance in the crystalline state should be considerably shorter than that obtained by us. From the small numbers of experimental gas phase studies it was argued that there are no strong arguments for expecting much longer charge-transfer distances in gas phase than in the crystalline state. Later, a microwave study of the  $\text{NH}_3\cdots\text{Cl}_2$  complex has been published,<sup>5</sup> which indicate that the  $\text{N}\cdots\text{Cl}$  distance may be considerably longer than that anticipated from the X-ray structures and even longer than that found in our study. Although it seems difficult to assess the uncertainties in this microwave result, the result makes our earlier conclusions on this point somewhat questionable.

Crystal structures have been reported for several complexes between oxygen-containing molecules and  $\text{Cl}_2$ ,  $\text{Br}_2$ , or  $\text{I}_2$ .<sup>6</sup>

These structures show intermolecular bonds which are considerably longer than those observed in amine–halogen complexes. This trend is opposite to that observed for hydrogen bond distances to oxygen and nitrogen.<sup>7</sup> In all the structures the halogen molecule points approximately toward a lone pair of the oxygen atom. Very few ab initio quantum mechanical studies of complexes of oxygen-containing molecules with halogens have been reported so far. In a study of the complex  $\text{H}_2\text{O}\cdot\text{Cl}_2$ , using the SCF model with a split valence 4-31G basis set, La Grange, Leroy, and Louterman-Leloup found a geometry with both Cl atoms in the plane of the  $\text{H}_2\text{O}$  molecule to be the most stable.<sup>8</sup> The same type of geometry was found for the  $\text{H}_2\text{O}\cdot\text{F}_2$  complex by Reed, Weinhold, Curtiss, and Pochatko using the computational model MP2/6-31G\*.<sup>9</sup> From spectroscopic measurements in solution energies of formation have been calculated for halogen complexes with oxygen-containing molecules, which are smaller than for those with amines.<sup>10</sup>

In this paper we report the results of a quantum mechanical study of complexes between  $\text{H}_2\text{O}$  and  $\text{F}_2$ ,  $\text{Cl}_2$ , and  $\text{ClF}$ , based on a similar computational model as that used for the complexes with  $\text{NH}_3$ . For the complex with  $\text{Cl}_2$  it seems relevant to compare the geometry with that observed in the crystal structure of the complex between dioxane and  $\text{Cl}_2$ ,<sup>11</sup> as crystal structures indicate that charge-transfer bond distances to a certain halogen is approximately the same for different oxygen-containing molecules. However, in the dioxane· $\text{Cl}_2$  structure both chlorine atoms are involved in an endless chain of charge-transfer bonds, whereas our calculations are on an isolated complex.

The purpose of this work is 3-fold: (1) compare the distance and direction of the oxygen–chlorine bond obtained for the  $\text{H}_2\text{O}\cdot\text{Cl}_2$  complex with those in the crystalline dioxane· $\text{Cl}_2$

(6) Prout, C. K.; Kamenar, B. In *Molecular Complexes*; Foster, R., Ed.; Elek: London, 1973; Vol. 1, Chapter 3.

(7) Olovsson, I.; Jönsson, P.-G. In *The Hydrogen Bond. Vol. II*; Schuster, P., Zundel, G., Sandorfy, C., Eds.; North-Holland: Amsterdam, 1976.

(8) La Grange, J.; Leroy, G.; Louterman-Leloup, G. *Bull. Soc. Chim. Belg.* **1977**, *86*, 241.

(9) Reed, A. E.; Weinhold, F.; Curtiss, L. A.; Pochatko, D. J. *J. Chem. Phys.* **1986**, *84*, 5687.

(10) Foster, R. *Organic Charge-Transfer Complexes*; Academic Press: London, 1969.

(11) Hassel, O.; Strømme, K. O. *Acta Chem. Scand.* **1959**, *13*, 1775.

<sup>⊗</sup> Abstract published in *Advance ACS Abstracts*, April 15, 1996.

(1) Mulliken, R. S. *J. Am. Chem. Soc.* **1952**, *74*, 811.

(2) Hanna, M. W.; Lippert, J. L. In *Molecular Complexes*; Foster, R., Ed.; Elek: London, 1973; Vol. 1, Chapter 1.

(3) Mulliken, R. S.; Person, W. B. *J. Am. Chem. Soc.* **1969**, *91*, 3409.

(4) Røeggen, I.; Dahl, T. *J. Am. Chem. Soc.* **1992**, *114*, 511.

(5) Legon, A. C.; Lister, D. G.; Thorn, J. C. *Chem. Commun.* **1994**, 957.

complex; (2) compare the intermolecular distances and bonding energies obtained for the complexes with those obtained for complexes of NH<sub>3</sub> with the same partner molecules; (3) on the basis of the results to describe the nature of the bonding in the complexes and the differences in the bonding between these complexes and those of NH<sub>3</sub>.

## II. Theoretical Framework

The theoretical framework is based on a recently constructed extended group function (EXGF) model.<sup>12</sup> This new model is a generalization of the extended geminal models used previously in this research program on intermolecular interactions. In this section we sketch the essential elements of the new model.

The extended group function model used in this study has the following form:

$$E^{\text{EXGF}} = E^{\text{RHF}} + \sum_{s=1}^{N_{\text{Sub}}} E_{\text{corr}}^s + \sum_{s<t}^{N_{\text{Sub}}} E_{\text{corr}}^{s,t} \quad (1)$$

In (1)  $E^{\text{RHF}}$  denotes the restricted Hartree–Fock (RHF) energy of the complex,  $E_{\text{corr}}^s$  is the correlation energy of subsystem  $s$ , when the other subsystems are described by an RHF approximation. Similarly,  $E_{\text{corr}}^{s,t}$  is the intersystem correlation energy for the subsystems  $s$  and  $t$  when the other subsystems are described by an RHF approximation. In this work  $E_{\text{corr}}^s$  corresponds to Möller–Plesset third order perturbation theory:

$$E_{\text{corr}}^s = E_{\text{MP3}}^s \quad (2)$$

The intersystem correlation energy is approximated by a sum of double pair correction terms as defined in the extended group function model:<sup>12</sup>

$$E_{\text{corr}}^{s,t} = \sum_{K=1}^{N_s} \sum_{L=1}^{N_t} \epsilon_{s,K;t,L} \quad (3)$$

In this particular model the double pair correction term is written as

$$E_{\text{corr}}^{s,t} = \sum_{K=1}^{N_s} \sum_{L=1}^{N_t} \{ \epsilon_{s,K;t,L}^{(2)} + \epsilon_{s,K;t,L}^{(3)} \} \quad (4)$$

The term  $\epsilon_{s,K;t,L}^{(2)}$  is a dispersion type correction and  $\epsilon_{s,K;t,L}^{(3)}$  is full CI correction.<sup>13</sup>

Triple-pair correlation corrections are neglected in this work since they have a negligible effect on the potential of the complexes in question.

Since triple-pair corrections are neglected in this work, the difference between the adopted EXGF model for the present calculations and the EXGEM model used in our previous study of the complexes between NH<sub>3</sub> and F<sub>2</sub>, Cl<sub>2</sub> and ClF,<sup>4</sup> is the calculation of the intrasystem correlation energy. The sum of single pair correction terms is replaced by Möller–Plesset third order perturbation theory.

Localized RHF-orbitals are obtained by minimizing the Coulomb repulsion between the associated electron pairs. Two concepts are used to characterize the localization of the orbitals: the charge centroid and the charge ellipsoid of an orbital. The charge centroids are a set of vectors which are

defined on the basis of the expression for the electronic part of the electric dipole moment. A straightforward derivation leads to the following well-known relations:

$$\langle \Phi^{\text{RHF}} | - \sum_{i=1}^{2N} \mathbf{r}_i \Phi^{\text{RHF}} \rangle = -2 \sum_{K=1}^N \langle \phi^K | \mathbf{r} \phi^K \rangle = -2 \sum_{K=1}^N \mathbf{r}^K \quad (5)$$

The vector  $\mathbf{r}^K$  is the average position, or the charge centroid, of the electrons associated with the RHF orbital  $\phi^K$ . Following Robb et al.<sup>14</sup> and Csizmadia<sup>15</sup> we define a measure of the extension of the geminal one-electron density by means of the second-order moments of the position operator, using the charge centroid as a local origin. The second-order moments (or variance matrix) associated with the orbital  $\phi^K$  are defined by the relations

$$M_{rs}^K = \langle \phi^K | (x_r - x_r^K)(x_s - x_s^K) | \phi^K \rangle \quad r,s \in \{1,2,3\} \quad (6)$$

where  $x_r^K$  is the  $r$ th component of the charge-centroid vector  $\mathbf{r}^K$  defined in (5). Diagonalization of the variance matrix yields the charge ellipsoid. The eigenvalues  $\{a_1, a_2, a_3\}$  of the matrix ( $M_{rs}^K$ ) correspond to the squares of the half-axes of the ellipsoid. The standard deviations in three orthogonal directions are therefore given by

$$\Delta l_i = a_i^{1/2} \quad i \in \{1,2,3\} \quad (7)$$

The quantities  $\{\Delta l_i\}$  can then be used as a measure of the extension of the geminal one-electron density. Furthermore, we may also use the volume of the ellipsoid as a single number of the extension of the geminal one-electron density:

$$V = \frac{4}{3} \pi \Delta l_1 \Delta l_2 \Delta l_3 \quad (8)$$

By using the localization measures, introduced in the previous paragraph, a molecular system can be partitioned into fragments or subsystems. Electron pairs and the nuclei belonging to a given fragment are localized in the same part of the physical space. Within the framework of the EXGF models, the total energy in the absence of nuclear motion, can be written as a sum of intra- and intersystem energies:

$$E_{\text{supersystem}}^{\text{EXGF}} \equiv E^{\text{EXGF}} + E_{\text{nuc}} \\ E^{\text{EXGF}} = \sum_s E^s + \sum_{s<t} E^{s,t} \quad (9)$$

where  $E^{\text{EXGF}}$  is given by (1),  $E_{\text{nuc}}$  denotes the nuclear electrostatic energy, and  $E^s$  and  $E^{s,t}$  are the intra- and intersystem energies, respectively. The intersystem energy between subsystems  $s$  and  $t$  is given by

$$E^{s,t} = E_{\text{coul}}^{s,t} + E_{\text{exch}}^{s,t} + E_{\text{corr}}^{s,t}$$

We obtain the following expression for the intermolecular potential  $\mathbf{U}$ :

(14) Roble, M. A.; Haines, W. J.; Csizmadia, I. G. *J. Am. Chem. Soc.* **1973**, *95*, 42.

(15) Csizmadia, I. G. In *Localization and Delocalization in Quantum Chemistry*; Chalvet, O., Daudel, R., Diner, S., Malbrieu, J. P., Eds.; D. Reidel: Dordrecht, Holland, 1975.

(12) Røeggen, I.; Ahmadi, G. R.; Wind, P. A. *J. Chem. Phys.* **1993**, *99*, 227.

(13) Røeggen, I. *Int. J. Quantum Chem.* **1990**, *37*, 585.

$$\begin{aligned}
 \mathbf{U} &= E_{\text{supersystem}}^{\text{EXGF}} - \sum_s E_{\text{isolated}}^s \quad (10) \\
 &= \sum_s \{E_{\text{supersystem}}^s - E_{\text{isolated}}^s\} + \sum_{s < t} E^{s,t} \\
 &= \Delta_{\text{dist}} + \Delta_{\text{int}} \\
 &= \sum_s \tilde{\Delta}_{\text{dist}}^s + \sum_{s < t} \{\Delta_{\text{coul}}^{s,t} + \Delta_{\text{exch}}^{s,t} + \Delta_{\text{corr}}^{s,t}\}
 \end{aligned}$$

In this equation  $\Delta_{\text{dist}}^s$  is the distortion energy of the subsystem  $s$  due to the presence of other subsystems. The interaction energy  $\Delta_{\text{int}}$  is simply the sum of the Coulombic, exchange, and correlation parts in (10).

As in our previous work<sup>4</sup> we introduce a modified partitioning scheme. In this scheme the Coulombic intersystem interaction is written as a sum of an electrostatic term and an induction term:

$$\Delta_{\text{ind}}^{s,t} = \Delta_{\text{coul}}^{s,t} - \Delta_{\text{elstat}}^{s,t} \quad (11)$$

The exchange terms are included in a set of modified distortion terms:

$$\tilde{\Delta}_{\text{dist}}^s = \Delta_{\text{dist}}^s + \frac{1}{2} \sum_{t \neq s} \Delta_{\text{exch}}^{s,t} \quad (12)$$

As a result we have the following modified decomposition scheme:

$$U = \sum_s \tilde{\Delta}^s + \sum_{s < t} (\Delta_{\text{elstat}}^{s,t} + \Delta_{\text{ind}}^{s,t} + \Delta_{\text{corr}}^{s,t}) \quad (13)$$

### III. Computational Details

Two different basis sets are used in this work. The smaller set, denoted basis A, are contracted Gaussian type functions (GTFs) [4s,2p], [7s,4p,2d], and [9s,6p,2d] for hydrogen, oxygen/fluorine, and chlorine, respectively. The hydrogen, fluorine, and chlorine sets are identical to the basis sets used in our previous studies<sup>4</sup> on the complexes H<sub>3</sub>N•F<sub>2</sub>, H<sub>3</sub>N•Cl<sub>2</sub>, and H<sub>3</sub>N•ClF. The oxygen set is constructed by the same procedure as defined in the quoted reference. The larger set, denoted basis B, comprises contracted GTFs [4s,3p,1d], [8s,5p,4d,2f], and [9s,6p,4d,2f] for hydrogen, oxygen/fluorine, and chlorine, respectively. For hydrogen the  $s$ -type functions are identical to the set in basis A. The exponents of the uncontracted polarization functions are {0.8, 0.32, 0.128/0.2429}. In constructing the  $s$ - and  $p$ -type sets for oxygen/fluorine we start from an uncontracted (9s,5p) (ref 16, Tables 8.65.1 and 9.63.1). This set is contracted to [6s,4p], keeping the most diffuse functions uncontracted. The  $s$ -type functions are further augmented with two diffuse  $s$ -type functions defined as an even tempered extension of the original set. For the  $p$ -type functions one extra set of diffuse functions is added. The exponents of the polarization functions are determined according to the procedure introduced by Ahlrichs and Taylor.<sup>17</sup> The exponents are respectively {2.0239, 0.8095, 0.3238, 0.1295/1.5360, 0.2457} and {2.5414, 1.0246, 0.4098, 0.1639, / 1.9440, 0.3110} for oxygen and fluorine. The  $s$ - and  $p$ -type sets for chlorine are identical to the corresponding sets in basis A. The exponents of the polarization functions are determined according to the Ahlrichs–Taylor procedure.<sup>17</sup> As a result we have the following exponents for the polarization functions {0.9787, 0.3915, 0.1566, 0.0626 / 0.7428, 0.1188}.

(16) Poirier, R.; Kari, R.; Csiszmadia, I. G. *Physical Sciences Data 24, Handbook of Gaussian Basis Sets*; Elsevier: Amsterdam, 1985.

(17) Ahlrichs, R.; Taylor, P. R. *J. Chem. Phys.* **1981**, 78, 316.

**Table 1.** Calculated Equilibrium Structures and Total Energies and Experimental Structures for the Isolated Molecules H<sub>2</sub>O, F<sub>2</sub>, Cl<sub>2</sub>, and ClF

molecule	model	$r_e$ (Å)	$\angle\text{HOH}$ (deg)	$E^{\text{EXGF}}$ (au)
H <sub>2</sub> O	MP2/basis A (all electrons)	0.967	103.7	-76.298 850
	MP3/basis B (valence electrons)	0.960	104.6	-76.326 036
	Experimental <sup>a</sup>	0.9575	104.51	
F <sub>2</sub>	MP3/basis B (valence electrons)	1.389		-199.279 280
	Experimental <sup>b</sup>	1.4119		
Cl <sub>2</sub>	MP2/basis A (all electrons)	2.039		-919.468 035
	MP3/basis B (valence electrons)	2.008		-919.403 855
	Experimental <sup>c</sup>	1.9885		
ClF	MP2/basis A (valence electrons)	1.666		-559.358 835
	MP3/basis B (valence electrons)	1.631		-559.362 406
	Experimental <sup>d</sup>	1.632		

<sup>a</sup> References 23 and 24. <sup>b</sup> References 25 and 26. <sup>c</sup> Reference 27. <sup>d</sup> Reference 28.

In all calculations we are using the Beebe–Linderberg two-electron integral approximation.<sup>18,19</sup> We select an integral threshold  $\delta = 10^{-7}$  au. Test calculations on the HF molecule demonstrate that by using this integral threshold, the errors in the calculated energy should be less than  $10^{-6}$  au.

All intersystem double-pair correction terms  $\{\epsilon_{KL}^{(2)}\}$  are defined in terms of 82 dispersion type natural orbitals (NOs). The full CI corrections  $\{\epsilon_{KL}^{(3)}\}$  are calculated in an orbital subspace consisting of 34 NOs. For the equilibrium structures, using basis B, the full CI correction corresponds to respectively 9.2%, 5.0%, and 7.2% of the total intersystem correlation energy for H<sub>2</sub>O•F<sub>2</sub>, H<sub>2</sub>O•ClF and H<sub>2</sub>O•Cl<sub>2</sub>.

The basis set superposition error (BSSE) at the correlation level is practically eliminated by the procedure introduced by Røeggen and Skullerud.<sup>20</sup> There is a small BSSE at the RHF level. Estimated by the Boys–Bernardi counterpoise procedure,<sup>21</sup> we find that for H<sub>2</sub>O•ClF, equilibrium structure, and using basis B, this error is 0.000 384 au. Similar errors are expected for the other two complexes in question.

### IV. Results

**(A) Equilibrium Structures.** Geometries of the molecules from geometry optimization of the isolated molecules were used in all calculations, except those for the H<sub>2</sub>O•ClF complex with basis B. In the latter calculations also the Cl–F bond distance was varied, starting with the geometry optimized distance of the isolated molecule. The optimized geometries of the isolated molecules are shown in Table 1. All equilibrium geometries of the complexes were obtained by a parabolic fit, except that for H<sub>2</sub>O•ClF with basis set B, where a two-dimensional quadratic fit was used. The equilibrium geometries appear from Table 2 and Figure 1. The equilibrium Cl–F bond distance in the complex obtained with basis B is 1.462 Å, 0.011 Å longer than that in the isolated molecule. The variation of this distance turned out to have small effects on the equilibrium geometry and the bonding energy of the complex. Using basis set A for the H<sub>2</sub>O•F<sub>2</sub> complex an unreasonable geometry was obtained,

(18) Beebe, N. H. F.; Linderberg, J. *Int. J. Quantum Chem.* **1977**, 12, 683.

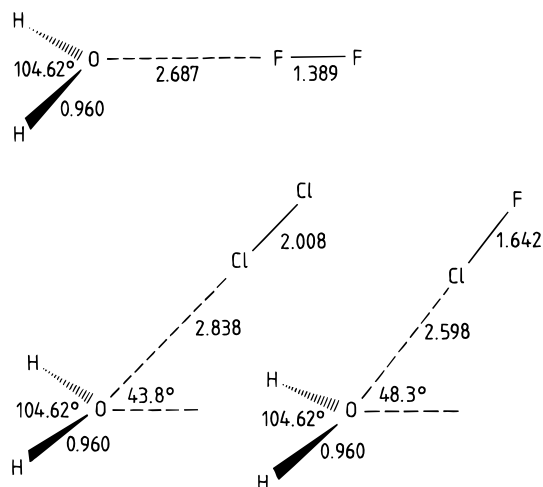
(19) Røeggen, I.; Wisløff-Nilssen, E. *Chem. Phys. Lett.* **1986**, 132, 254.

(20) Røeggen, I.; Skullerud, H. *J. Phys. B.: At Mol. Opt. Phys.* **1992**, 25, 1795.

(21) Boys, S. F.; Bernardi, F. *Mol. Phys.* **1970**, 19, 553.

**Table 2.** Optimized Geometries of the Complexes  $\text{H}_2\text{O}\cdot\text{F}_2$ ,  $\text{H}_2\text{O}\cdot\text{Cl}_2$ ,  $\text{H}_2\text{O}\cdot\text{ClF}$ , and Binding Energies<sup>a</sup>

model	$R(\text{O} \cdots \text{X})/\text{\AA}$	$\alpha/\text{deg}$	$D_e/\text{kJ mol}^{-1}$
$\text{H}_2\text{O}\cdot\text{F}_2$			
EXGF/MP3-D/basis B	2.69	0	5.86
$\text{H}_2\text{O}\cdot\text{Cl}_2$			
EXGF/MP2-D/basis A	2.88	40.0	11.08
EXGF/MP3-D/basis B	2.84	43.8	12.51
$\text{H}_2\text{O}\cdot\text{ClF}$			
EXGF/MP2-D/basis A	2.65	53.3	19.43
EXGF/MP3-D/basis B	2.60	48.3	20.24

<sup>a</sup> See Figure 2 for definition of parameters.**Figure 1.** Equilibrium structures of the EDA complexes studied in this work. (Distances in  $\text{\AA}$ .)

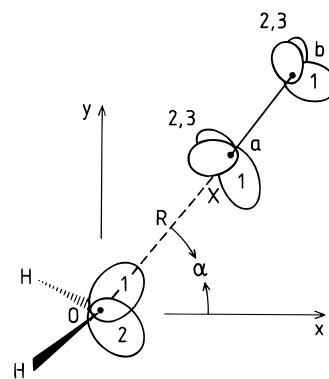
probably an artefact due to small basis set. These results are therefore not included in Tables 1–4.

The equilibrium intermolecular distances obtained with basis set B are shorter than those obtained with basis A. The discussions below are based on the results obtained by basis B.

In the  $\text{H}_2\text{O}\cdot\text{F}_2$  complex the oxygen—halogen bond is in the plane of the  $\text{H}_2\text{O}$  molecule. In the  $\text{H}_2\text{O}\cdot\text{ClF}$  complex the angle between this plane and the corresponding bond is nearly such that the halogen molecule points directly toward a lone pair of the oxygen atom. In the  $\text{H}_2\text{O}\cdot\text{Cl}_2$  complex this angle is slightly smaller. The latter result is in relatively good agreement with that found for the crystal structure of the dioxane $\cdot\text{Cl}_2$  complex,<sup>11</sup> where the corresponding angle is  $5^\circ$  smaller than that obtained for the  $\text{H}_2\text{O}\cdot\text{Cl}_2$  complex in the present study.

In the complexes with  $\text{Cl}_2$  and  $\text{ClF}$  the equilibrium intermolecular distances are 0.24 and 0.30  $\text{\AA}$ , respectively, longer than those found for the complexes of  $\text{NH}_3$  with the same acceptor molecules. The O—Cl distance in the  $\text{H}_2\text{O}\cdot\text{Cl}_2$  complex is 0.15  $\text{\AA}$  longer than that observed in the crystal structure of the dioxane $\cdot\text{Cl}_2$  complex. The intermolecular distance in the  $\text{H}_2\text{O}\cdot\text{F}_2$  complex is slightly shorter than that in the  $\text{H}_3\text{N}\cdot\text{F}_2$  complex. In both these  $\text{F}_2$  complexes the distance is not much shorter than the van der Waals distance between the partner molecules.<sup>22</sup>

For the  $\text{H}_2\text{O}\cdot\text{F}_2$  complex the direction of the O—F bond is the same, and the equilibrium bond distance is 0.08  $\text{\AA}$  longer than that obtained by MP2 calculations by Reed, Weinhold, Curtiss, and Pochatko.<sup>9</sup> The equilibrium distance of the O—Cl bond in the  $\text{H}_2\text{O}\cdot\text{Cl}_2$  complex is 0.11  $\text{\AA}$  longer, and the direction of the bond deviates strongly from that found by La Grange, Leroy, and Louterman-Leloup.<sup>6</sup> This deviation may be a result of a small basis set and the neglect of electron correlation in the model of the latter authors.

**Figure 2.** Figure defining parameters, coordinates, and subscripts for atoms and lone pair geminals used in the tables.

**(B) Energy Decomposition.** The energy decomposition for the equilibrium structures based on the primary partition scheme is presented in Table 3. The magnitude of the potential at the equilibrium geometry for the  $\text{F}_2$  complex is only slightly smaller than for the corresponding complex with  $\text{NH}_3$ , whereas those for the  $\text{Cl}_2$  and the  $\text{ClF}$  complexes are approximately half as large as for the corresponding  $\text{NH}_3$  complexes. As also found for the corresponding  $\text{NH}_3$  complexes, the stabilities and thus also the magnitudes of the different contributions are smallest for the  $\text{H}_2\text{O}\cdot\text{F}_2$  complex and largest for the  $\text{H}_2\text{O}\cdot\text{ClF}$  complex.

Apart from this difference between the  $\text{H}_2\text{O}$  complexes, the most striking difference is that the distortion energy of the water molecule is much more dominant and that of the halogen molecule much less dominant for the  $\text{F}_2$  complex than for the two other complexes. In all complexes the distortion energy of the donor molecule is more dominant than in the complexes of  $\text{NH}_3$  with the same acceptor molecules. The magnitudes of both of the potential and all the components obtained with basis B are larger than those obtained with basis A. The largest difference is found for the correlation energy. When basis B is used, the Coulombic term, the distortion term, and the exchange term partly cancel each other in all complexes, so that the intersystem correlation term is relatively close to the potential. A similar result was obtained for the  $\text{NH}_3$  complexes.

The energy decomposition based on the Modified Partition Scheme is presented in Table 4. It appears that the ratio  $\Delta_{\text{ind}}/\Delta_{\text{elstat}}$  is considerably larger for the  $\text{F}_2$  complex than for the two other complexes. The ratios  $\Delta_{\text{ind}}/\Delta_{\text{elstat}}$  in the latter complexes are relatively equal and much smaller than in the corresponding  $\text{NH}_3$  complexes. They are, however, larger than the corresponding ratios in the hydrogen-bonded complexes  $(\text{HF})_2$ ,  $(\text{H}_2\text{O})_2$ , and  $\text{H}_2\text{O}\cdot\text{HF}$ .<sup>4</sup> This result seems therefore to confirm the conjecture put forward earlier<sup>4</sup> that this ratio is larger in charge-transfer complexes than in hydrogen-bonded complexes.

The variation of the energy components obtained with basis B as a function of the direction of the intermolecular bond appear from Tables 5 and 6. The magnitude of all components increase with increasing angle between this bond and the plane of the  $\text{H}_2\text{O}$  molecule.

**(C) Changes in the One-Electron Density.** For the changes of the one-electron densities only results obtained with basis B are presented. As an overall measure of these changes during formation of the complexes, the changes of the electric dipole moments of the subsystems are considered. The electric dipole moments are calculated at the RHF level and are presented in Table 7.

In all complexes there is a shift of the electronic charge density in the direction from the  $\text{H}_2\text{O}$  molecule to the halogen molecule. For the  $\text{H}_2\text{O}$  molecule the change increases consider-

(22) Bondi, A. *J. Phys. Chem.* **1964**, *68*, 441.

**Table 3.** Partitioning of the Intermolecular Potential for the Equilibrium Structures Using the Primary Partitioning Scheme<sup>a-c</sup>

	H <sub>2</sub> O•F <sub>2</sub>	H <sub>2</sub> O•Cl <sub>2</sub>		H <sub>2</sub> O•ClF	
	basis B	basis A	basis B	basis A	basis B
$\Delta_{\text{dist}}^{\text{d}}$	0.006 547 (70.5%)	0.011 620 (56.6%)	0.013 145 (56.1%)	0.029 622 (60.2%)	0.032 713 (59.5%)
$\Delta_{\text{dist}}^{\text{a}}$	0.002 740 (29.5%)	0.008 903 (43.4%)	0.010 267 (43.9%)	0.019 594 (39.8%)	0.022 241 (40.5%)
$\Delta_{\text{coul}}^{\text{a,d}}$	-0.007 836 (-84.4%)	-0.017 771 (-86.6%)	-0.019 478 (-83.2%)	-0.042 575 (-86.5%)	-0.046 111 (-83.9%)
$\Delta_{\text{exch}}^{\text{a,d}}$	-0.001 845 (-19.9%)	-0.004 094 (-19.9%)	-0.004 680 (-20.0%)	-0.009 433 (-19.2%)	-0.010 355 (-18.8%)
$\Delta_{\text{corr}}^{\text{a,d}}$	-0.001 836 (-19.8%)	-0.002 877 (-14.0%)	-0.004 017 (-17.2%)	-0.004 607 (-9.4%)	-0.006 198 (-11.3%)
$U$	-0.002 231 (-24.0%)	-0.004 220 (-20.6%)	-0.004 763 (-20.3%)	-0.007 400 (-15.0%)	-0.007 709 (-14.0%)

<sup>a</sup> Atomic units. <sup>b</sup> The superscripts d and a refer to the “donor” and “acceptor” subsystems, respectively. <sup>c</sup> Numbers in parentheses are based on the sum of the repulsive terms as energy unit.

**Table 4.** Partitioning of the Intermolecular Potential for the Equilibrium Structures Using the Modified Partitioning Scheme<sup>a-c</sup>

	H <sub>2</sub> O•F <sub>2</sub>	H <sub>2</sub> O•Cl <sub>2</sub>		H <sub>2</sub> O•ClF	
	basis B	basis A	basis B	basis A	basis B
$\tilde{\Delta}_{\text{dist}}^{\text{d}}$	0.005 624 (75.6%)	0.009 573 (58.3%)	0.010 806 (57.7%)	0.024 906 (62.6%)	0.027 536 (61.7%)
$\tilde{\Delta}_{\text{dist}}^{\text{a}}$	0.001 817 (24.4%)	0.006 856 (41.7%)	0.007 927 (42.3%)	0.014 878 (37.4%)	0.017 064 (38.3%)
$\Delta_{\text{elstat}}^{\text{a,d}}$	-0.001 899 (-25.5%)	-0.006 194 (-37.7%)	-0.006 635 (-35.4%)	-0.013 242 (-33.3%)	-0.013 978 (-31.3%)
$\Delta_{\text{ind}}^{\text{a,d}}$	-0.005 936 (-79.8%)	-0.011 577 (-70.5%)	-0.012 844 (-68.6%)	-0.029 333 (-73.7%)	-0.032 133 (-72.0%)
$\Delta_{\text{corr}}^{\text{a,d}}$	-0.001 836 (-24.7%)	-0.002 877 (-17.5%)	-0.004 017 (-21.4%)	-0.004 607 (-11.6%)	-0.006 198 (-13.9%)
$U$	-0.002 231 (-30.0%)	-0.004 220 (-25.7%)	-0.004 763 (-25.4%)	-0.007 400 (-18.6%)	-0.007 709 (-17.3%)

<sup>a</sup> Atomic units. <sup>b</sup> See footnote b, Table 3. <sup>c</sup> Numbers in parentheses are based on the sum of the repulsive terms as energy unit.

**Table 5.** Changes of Energy Components as Function of the Angle  $\alpha$ , Using the Primary Partitioning Scheme<sup>a-d</sup>

$\alpha$ / deg	H <sub>2</sub> O•F <sub>2</sub> $R = 5.15$ au				H <sub>2</sub> O•Cl <sub>2</sub> $R = 5.3667$ au			H <sub>2</sub> O•ClF $R = 4.9067$ au			
	0.0	15.0	30.0	45.0	37.7	45.0	52.0	40.0	47.0	53.3	60.0
$\Delta_{\text{dist}}^{\text{d}}$	0.005 690 (70.9%)	0.005 843 (70.5%)	0.006 286 (69.9%)	0.006 968 (69.8%)	0.012 635 (56.1%)	0.013 161 (56.2%)	0.013 729 (56.4%)	0.031 337 (59.3%)	0.032 631 (59.5%)	0.033 904 (59.8%)	0.035 339 (60.2%)
$\Delta_{\text{dist}}^{\text{a}}$	0.002 336 (29.1%)	0.002 443 (29.5%)	0.002 704 (30.1%)	0.003 018 (30.2%)	0.009 888 (43.9%)	0.010 268 (43.8%)	0.010 596 (43.6%)	0.021 488 (40.7%)	0.022 227 (40.5%)	0.022 839 (40.2%)	0.023 404 (39.8%)
$\Delta_{\text{coul}}^{\text{a,d}}$	-0.006 948 (-86.6%)	-0.007 123 (-86.0%)	-0.007 606 (-84.6%)	-0.008 281 (-82.9%)	-0.018 853 (-83.7%)	-0.019 488 (-83.2%)	-0.020 088 (-82.6%)	-0.044 495 (-84.2%)	-0.046 039 (-83.9%)	-0.407 416 (-83.6%)	-0.048 803 (-83.1%)
$\Delta_{\text{exch}}^{\text{a,d}}$	-0.001 614 (-20.1%)	-0.001 659 (-20.0%)	-0.001 785 (-19.9%)	-0.001 966 (-19.7%)	-0.004 493 (-19.9%)	-0.004 686 (-20.0%)	-0.004 882 (-20.1%)	-0.009 930 (-18.8%)	-0.010 330 (-18.8%)	-0.010 706 (-18.9%)	-0.011 109 (-18.9%)
$\Delta_{\text{corr}}^{\text{a,d}}$	-0.001 684 (-21.0%)	-0.001 698 (-20.5%)	-0.001 741 (-19.4%)	-0.001 806 (-18.1%)	-0.003 934 (-17.5%)	-0.004 016 (-17.1%)	-0.004 107 (-16.9%)	-0.006 072 (-11.5%)	-0.006 198 (-11.3%)	-0.006 317 (-11.1%)	-0.006 449 (-11.0%)
$U$	-0.002 220 (-27.7%)	-0.002 194 (-26.5%)	-0.002 141 (-23.8%)	-0.002 067 (-20.7%)	-0.004 757 (-21.1%)	-0.004 762 (-20.3%)	-0.004 753 (-19.5%)	-0.007 673 (-14.5%)	-0.007 709 (-14.1%)	-0.007 696 (-13.6%)	-0.007 619 (-13.0%)

<sup>a</sup> Atomic units. <sup>b</sup> See footnote b, Table 3. <sup>c</sup> See Figure 2 for definition of parameters. <sup>d</sup> Numbers in parentheses are based on the sum of the repulsive terms as energy unit.

ably by going from the F<sub>2</sub> complex to the ClF complex. These changes are, however, considerably less than those found for NH<sub>3</sub> in the corresponding NH<sub>3</sub> complexes. For the halogen molecule the relative changes in the dipole moment in the three complexes are more equal. For the Cl<sub>2</sub> and the ClF complexes these changes are slightly more than 50% of those found in the NH<sub>3</sub> complexes, whereas for the F<sub>2</sub> complex the change is larger than that found for the NH<sub>3</sub> complex.

The changes of the charge centroids of selected geminals in the two complexes are given in Table 8. As also observed for the NH<sub>3</sub> complexes there are large changes in one lone pair of the donor molecule in the Cl<sub>2</sub> and ClF complexes but not in the F<sub>2</sub> complex. The large change in the Cl<sub>2</sub> and ClF complexes is observed for the lone pair pointing approximately in the

oxygen-halogen direction. This change is approximately twice as large in the ClF complex as in the Cl<sub>2</sub> complex. The largest change in the acceptor system of the F<sub>2</sub> and Cl<sub>2</sub> complexes is in the bond pair. The change along the halogen-halogen bond for the Cl<sub>2</sub> complex is approximately the same and for the F<sub>2</sub> complex considerably larger than for the corresponding geminals in the NH<sub>3</sub> complexes. As the geometry of the ClF molecule in the complex is different from that of the isolated molecule, the changes of the charge centroids in this molecule is not included in the table.

Details of the H<sub>2</sub>O lone pair ellipsoids in the three complexes are given in Table 9. For the lone pair pointing along the charge-transfer bond in the Cl<sub>2</sub> and ClF complexes there is an expansion in the longest half-axis and a contraction in the two

**Table 6.** Changes of Energy Components as Function of the Angle  $\alpha$ , Using the Modified Partitioning Scheme<sup>a–d</sup>

$\alpha$ / deg	$\text{H}_2\text{O}\cdot\text{F}_2 R = 5.15$ au				$\text{H}_2\text{O}\cdot\text{Cl}_2 R = 5.3667$ au			$\text{H}_2\text{O}\cdot\text{ClF} R = 4.9067$ au			
	0.0	15.0	30.0	45.0	37.7	45.0	52.0	40.0	47.0	53.3	60.0
$\bar{\Delta}_{\text{dist}}^{\text{d}}$	0.004 883 (76.2%)	0.005 013 (75.7%)	0.005 393 (74.9%)	0.005 985 (74.6%)	0.010 389 (57.6%)	0.010 818 (57.7%)	0.011 288 (58.1%)	0.026 372 (61.5%)	0.027 466 (61.7%)	0.028 551 (62.0%)	0.029 784 (62.5%)
$\bar{\Delta}_{\text{dist}}^{\text{a}}$	0.001 529 (23.8%)	0.001 613 (24.3%)	0.001 811 (25.1%)	0.002 035 (25.4%)	0.007 642 (42.4%)	0.007 925 (42.3%)	0.008 155 (41.9%)	0.016 523 (38.5%)	0.017 062 (38.3%)	0.017 486 (38.0%)	0.017 849 (37.5%)
$\Delta_{\text{elstat}}^{\text{a,d}}$	−0.001 721 (−26.8%)	−0.001 749 (−26.4%)	−0.001 825 (−25.3%)	−0.001 932 (−24.1%)	−0.006 495 (−36.0%)	−0.006 629 (−35.4%)	−0.006 751 (−34.7%)	−0.013 755 (−32.1%)	−0.013 990 (−31.4%)	−0.014 050 (−30.5%)	−0.014 339 (−30.1%)
$\Delta_{\text{ind}}^{\text{a,d}}$	−0.005 227 (−81.5%)	−0.005 374 (−81.1%)	−0.005 781 (−80.2%)	−0.006 349 (−79.2%)	−0.012 358 (−68.5%)	−0.012 859 (−68.6%)	−0.013 337 (−68.6%)	−0.030 740 (−71.7%)	−0.032 049 (−72.0%)	−0.033 367 (−72.5%)	−0.034 464 (−72.4%)
$\Delta_{\text{corr}}^{\text{a,d}}$	−0.001 684 (−26.3%)	−0.001 698 (−25.6%)	−0.001 741 (−24.2%)	−0.001 806 (−22.5%)	−0.003 934 (−21.8%)	−0.004 016 (−21.4%)	−0.004 107 (−21.1%)	−0.006 072 (−14.2%)	−0.006 198 (−13.9%)	−0.006 317 (−13.7%)	−0.006 449 (−13.5%)
$U$	−0.002 220 (−34.6%)	−0.002 194 (−33.1%)	−0.002 141 (−29.7%)	−0.002 067 (−25.8%)	−0.004 757 (−26.4%)	−0.004 762 (−25.4%)	−0.004 753 (−24.4%)	−0.007 673 (−17.9%)	−0.007 709 (−17.3%)	−0.007 696 (−16.7%)	−0.007 619 (−16.0%)

<sup>a</sup> Atomic units. <sup>b</sup> See footnote b, Table 3. <sup>c</sup> See Figure 2 for definition of parameters. <sup>d</sup> Numbers in parentheses are based on the sum of the repulsive terms as energy unit.

**Table 7.** Electric Dipole Moments of the Isolated Monomers and the Differences between the Corresponding Quantities in the Complex and the Isolated Monomer<sup>a</sup>

complex	monomer	$d^{\text{mon}}$	$d^{\text{comp}} - d^{\text{mon}}$
$\text{H}_2\text{O}\cdot\text{F}_2$	$\text{H}_2\text{O}$	0.7788	0.0123
	$\text{F}_2$	0	0.0915
$\text{H}_2\text{O}\cdot\text{Cl}_2$	$\text{H}_2\text{O}$	0.7788	0.0540
	$\text{Cl}_2$	0	0.2322
$\text{H}_2\text{O}\cdot\text{ClF}$	$\text{H}_2\text{O}$	0.7788	0.1070
	$\text{ClF}$	0.4408	0.2291

<sup>a</sup> Dipole moments in au.

**Table 8.** Changes of the  $x$  and  $y$  Components of the Charge Centroids of Selected Geminals of the Complexes Compared with the Corresponding Quantities of the Isolated Monomers<sup>a,b</sup>

complex	geminal	$x$	$y$
$\text{H}_2\text{O}\cdot\text{F}_2$	lone pairs of $\text{H}_2\text{O}$	0.0013	−0.0004
	bond pairs of $\text{H}_2\text{O}$	0.0018	0.0000
	lone pairs of $\text{F}_a$	0.0048	0.0000
	lone pairs of $\text{F}_b$	0.0029	0.0000
	bond pair of $\text{F}_2$	0.0225	0.0000
$\text{H}_2\text{O}\cdot\text{Cl}_2$	lone pair <sub>1</sub> of $\text{H}_2\text{O}$	0.0156	0.0118
	lone pair <sub>2</sub> of $\text{H}_2\text{O}$	0.0022	0.0027
	bond pairs of $\text{H}_2\text{O}$	0.0044	0.0024
	lone pair <sub>1</sub> of $\text{Cl}_a$	0.0124	0.0127
	lone pair <sub>2,3</sub> of $\text{Cl}_a$	0.0081	0.0128
	lone pair <sub>1</sub> of $\text{Cl}_b$	0.0047	0.0059
	lone pair <sub>2,3</sub> of $\text{Cl}_b$	0.0054	0.0057
$\text{H}_2\text{O}\cdot\text{ClF}$	bond pair of $\text{Cl}_2$	0.0318	0.0322
	lone pair <sub>1</sub> of $\text{H}_2\text{O}$	0.0306	0.0287
	lone pair <sub>2</sub> of $\text{H}_2\text{O}$	0.0043	0.0056
	bond pairs of $\text{H}_2\text{O}$	0.0082	0.0048

<sup>a</sup>  $x$  and  $y$  components in au. <sup>b</sup> See Figure 2 for definition of parameters and subscripts.

orthogonal directions. There is also an increase in volume of this ellipsoid in these complexes. Similar results were found for the nitrogen lone pair in the corresponding  $\text{NH}_3$  complexes. For the other lone pair of  $\text{H}_2\text{O}$  in the  $\text{Cl}_2$  and  $\text{ClF}$  complexes there is a contraction of the largest half-axis and a decrease in volume. For the lone pairs in the  $\text{F}_2$  complex there are only minor changes in the half-axes.

Details of the bond pair ellipsoids of the halogen acceptors are given in Table 10. There is a decrease in all the half-axes.

## V. Concluding Remarks

In this work we have shown that accurate quantum mechanical calculations on the  $\text{H}_2\text{O}$  complexes with  $\text{F}_2$ ,  $\text{Cl}_2$ , and  $\text{ClF}$  give smaller interaction energies than those obtained earlier for the corresponding  $\text{NH}_3$  complexes. For the complexes with  $\text{Cl}_2$  and  $\text{ClF}$  the intermolecular distances are longer than in the

**Table 9.** Half-Axes and Volume of the Charge Ellipsoids of the Lone Pair Geminals of Isolated  $\text{H}_2\text{O}$  and the Corresponding Lone Pair Geminals in the Complexes<sup>a–c</sup>

system	$\Delta l_1$	$\Delta l_2$	$\Delta l_3$	$V$
isolated $\text{H}_2\text{O}$	0.9221	0.7210	0.7102	1.9779
$\text{H}_2\text{O}\cdot\text{F}_2$ , lone pairs	0.9214	0.7196	0.7131	1.9806
	(−0.0007)	(−0.0014)	(0.0029)	(0.0027)
$\text{H}_2\text{O}\cdot\text{Cl}_2$ , lone pair <sub>1</sub>	0.9610	0.7163	0.7068	2.0382
	(0.0389)	(−0.0047)	(−0.0034)	(0.0603)
$\text{H}_2\text{O}\cdot\text{Cl}_2$ , lone pair <sub>2</sub>	0.9179	0.7186	0.7110	1.9644
	(−0.0042)	(−0.0024)	(0.0008)	(−0.0135)
$\text{H}_2\text{O}\cdot\text{ClF}$ , lone pair <sub>1</sub>	0.9759	0.7136	0.7032	2.0512
	(0.0538)	(−0.0074)	(−0.0070)	(0.0733)
$\text{H}_2\text{O}\cdot\text{ClF}$ , lone pair <sub>2</sub>	0.9126	0.7159	0.7107	1.9449
	(−0.0095)	(−0.0051)	(0.0005)	(−0.0330)

<sup>a</sup> Distances and volumes in atomic units. <sup>b</sup> See Figure 2 for definition of subscripts. <sup>c</sup> Differences in quantities with respect to the values for the isolated subsystem in parentheses.

**Table 10.** Half-Axes and Volume of the Charge Ellipsoid of the Bond Pair Geminal of the Halogen Acceptor Subsystem in the Complexes<sup>a,b</sup>

system	$\Delta l_1$	$\Delta l_2$	$\Delta l_3$	$V$
$\text{H}_2\text{O}\cdot\text{F}_2$ isolated	1.1754	0.5458	0.5458	1.4668
	complex	1.1715	0.5448	0.5446
	(−0.0039)	(−0.0010)	(−0.0012)	(−0.0108)
$\text{H}_2\text{O}\cdot\text{Cl}_2$ isolated	1.4621	0.8206	0.8206	4.1245
	complex	1.4503	0.8195	0.8192
	(−0.0118)	(−0.0011)	(−0.0014)	(−0.0464)
$\text{H}_2\text{O}\cdot\text{ClF}$ isolated	1.1644	0.6319	0.6319	1.9475
	complex	1.1560	0.6286	0.6284
	(−0.0084)	(−0.0033)	(−0.0035)	(−0.0348)

<sup>a</sup> Distances and volumes in atomic units. <sup>b</sup> Differences in quantities with respect to the values of the isolated subsystem in parentheses.

corresponding  $\text{NH}_3$  complexes. These trends are in accordance with those expected from experimental results.<sup>6,10</sup> The direction of the intermolecular bond in the  $\text{H}_2\text{O}\cdot\text{Cl}_2$  complex agrees well with that observed in the crystalline complex between dioxane and  $\text{Cl}_2$ .<sup>11</sup>

As polarization of the  $\text{Cl}_2$  molecule seems to be important in the  $\text{H}_2\text{O}\cdot\text{Cl}_2$  complex, it is surprising that the intermolecular distance obtained for this complex is longer than that observed in the endless chains in the crystalline dioxane· $\text{Cl}_2$  complex. Large effects of crystal forces may be a possible explanation of this finding.

(23) Cook, R. L.; DeLucia, F. C.; Helminger, P. *J. Mol. Spectrosc.* **1974**, *53*, 62.

(24) Benedict, W. S.; Gailar, N.; Plyler, E. K. *J. Chem. Phys.* **1956**, *24*, 1139.

(25) Peterson, K. A.; Kendall, R. A.; Dunning, T. H., Jr. *J. Chem. Phys.* **1993**, *99*, 9790.

The analysis of our results indicates that the H<sub>2</sub>O complexes with Cl<sub>2</sub> and ClF are of a similar nature. In these complexes one lone pair of the H<sub>2</sub>O molecule approaches a chlorine atom of the acceptor molecule. The direction of the intermolecular bond is mainly determined by this effect. In the complex with F<sub>2</sub> the fluorine nuclei are more effectively screened by the electrons. Subsequently the lone pairs of the H<sub>2</sub>O molecule are little involved in the complex formation. The intermolecular interaction in this complex seems to be more like a classical

(26) Huber, K. P.; Herzberg, G. *Molecular Spectra and Molecular Structure. IV. Constants of Diatomic Molecules*; Van Nostrand: Princeton, 1979.

(27) Edwards, H. G. M.; Long, D. A.; Mansour, H. R. *J. Chem. Soc., Faraday Trans. 2* **1978**, *74*, 1200.

(28) McGuirk, J.; Norris, C. L.; Tigelaar, H. L.; Flygare, W. H. *J. Chem. Phys.* **1973**, *58*, 3118.

van der Waals interaction, dominated by a relatively strong polarization of the F<sub>2</sub> molecule along its axis. The direction of the intermolecular bond is probably mainly determined by this polarization interaction.

Compared with the complexes of NH<sub>3</sub> with the same acceptor molecules the relative importance of the inductive component of the Coulombic energy is smaller in the complexes with H<sub>2</sub>O.

**Acknowledgment.** All calculations reported in this work were performed on the Cray X-MP216 supercomputer at RUNIT, Trondheim, Norway. This work was supported by the Norwegian Research Council for Science and Humanities and by the Norwegian Research Council.

JA9537890